

---

## OCEAN ACOUSTICS AND UNDERWATER ACOUSTICS

---

# Cross-Spectral Density Sensitivity Kernels in Surface Noise Field

Guangying Zheng<sup>a, b, \*</sup>, Yang Dong<sup>c, d, \*\*</sup>, You Shao<sup>a, b, \*\*\*</sup>,  
Hongsong Zhou<sup>a, b, \*\*\*\*</sup>, and Junyu Fu<sup>a, b, \*\*\*\*\*</sup>

<sup>a</sup>Science and Technology on Sonar Laboratory, Hangzhou, 310023 China

<sup>b</sup>Hangzhou Applied Acoustics Research Institute, Hangzhou, 310023 China

<sup>c</sup>Acoustic Science and Technology Laboratory, Harbin Engineering University, Harbin, 150001 China

<sup>d</sup>College of Underwater Acoustic Engineering, Harbin Engineering University, Harbin, 150001 China

\*e-mail: 276454158@qq.com

\*\*e-mail: dong\_yang@hrbeu.edu.cn

\*\*\*e-mail: jdsy1026@163.com

\*\*\*\*e-mail: zhouhongsong1990@163.com

\*\*\*\*\*e-mail: fujunyu1991@sina.com

Received October 10, 2018; revised November 11, 2019; accepted December 24, 2019

**Abstract**—The main factors affecting the spatial characteristics of surface noise fields are changes in sound speed and sea surface boundary perturbations due to mesoscale ocean phenomena and wind-induced noise, respectively. This study derived the surface noise cross-spectral density sensitivity kernel for sound speed changes and local boundary perturbations and analyzed their effects on cross-spectral density. Numerical results show that the sound speed perturbations of any position in the entire observation plane changes the surface noise cross-spectral density function in surface noise with finite frequency. The cross-spectral density between two receivers in the vertical direction is the most sensitive to the sound speed changes of the region between two receivers. Additionally, the influence depends on the relationship between the wavelength of sound wave and the distance of two receivers. Scattering on the surface boundary perturbation would lead to fluctuations in the cross-spectral density function. When the boundary perturbation along the horizontal direction is distant from two receivers, the cross-spectral density sensitivity kernel for surface scattering oscillates, and the influence of boundary perturbation on the cross-spectral density function gradually weakens. Finally, the period of the cross-spectral density sensitivity kernel oscillations is a half wavelength of the sound wave.

**Keywords:** surface noise field, cross-spectral density, sensitivity kernel, sound speed perturbation, boundary perturbation

**DOI:** 10.1134/S1063771020030100

## INTRODUCTION

As an interference of ocean acoustic channel, ocean ambient noise affects the detection performance of sonar systems. The optimization design of a sonar array can improve the detection performance of a sonar system by studying the spatial characteristics of the ocean's ambient noise field [1], which is a traditional content of ocean ambient noise research. Ocean ambient noise as an eternal field in ocean acoustics can provide various data about the ocean medium, such as the sound speed profile of a water column and information on the ocean bottom and surface. Some methods of obtaining medium information on the basis of the spatial characteristics of ocean ambient noise have been proposed. These methods include sound speed profile extraction [2], bottom geoaoustic parameter inversion [3–5], time-domain Green's function extraction [6–8], and passive fathometer

technique [9]. Ocean ambient noise is no longer a useless interference signal because it can provide marine medium information. Thus, studying ocean ambient noise may greatly improve our understanding of the marine medium.

The study of ocean ambient noise benefits from the design requirements of sonar arrays that originated from spatial coherence research (i.e., cross-spectral density function of ocean noise field [10]). On the basis of the ray model, Cron and Scherman [11] considered the deep sea as a homogeneous semi-infinite space, assumed the directivity  $\cos^p \theta$  of the sea surface noise source, established a deep-sea ambient noise model, and developed a prediction method of the horizontal and vertical correlation coefficients of the surface noise field. Based on this study, Chapman [12] derived the expressions of noise intensity and vertical

coherence function as functions of grazing angles. Kuperman and Ingenito [13] assumed that noise sources are randomly and continuously distributed on an infinite plane close to the sea surface. The noise propagation problem was studied on the basis of wave theory, the contribution of near-field continuous and far-field discrete spectra was considered, and the noise coherence function of a horizontal stratified waveguide was successfully predicted. Carey [14] used the parabolic equation method to study the ambient noise propagation in a range-dependent waveguide and predicted the vertical spatial characteristics of the noise field with a corresponding noise source model. Harrison [15] demonstrated that a simple ray approach can model sophisticated noise levels and coherence effects based on ray theory. This method is suitable for predicting high-frequency noise fields and compensates for the limitation of the normal mode and parabolic equation methods to a certain extent.

The spatial characteristics of noise fields have been studied in various media through different acoustic field modeling methods. At present, these spatial characteristics can be used to extract ocean medium information.

A simple method developed by Harrison and Simons uses vertically beamformed measurements of ocean ambient noise [5]. This method obtains a ratio between averaged noise directly from the seabed and that from the surface. In theory, bottom loss can be accurately estimated through this method, but the process requires perfect beamforming and averaging. These requirements imply an infinitely long hydrophone array (i.e., infinitely narrow beams) and infinite averaging time. A bottom loss estimate can be smoothed with finite hydrophone arrays due to beam widths, which are generally undesirable. Smoothing in a bottom loss estimate can shift the location of a critical angle or considerably reduce the level of interference fringes if the seabed is layered. Siderius and Harrison [16–18] proposed several methods to extrapolate the vertical coherence function, which can improve the accuracy of reflection loss extraction to a certain extent. Arnaud et al. [6] extracted the time-domain Green's function from the spatial correlation functions of ocean ambient noise. Meanwhile, a passive fathometer technique using ambient noise was developed by Siderius and Harrison [9]. The spatial characteristics of ocean ambient noise provide bottom information, which can be used for the inversion of bottom geoaoustic parameters. In real ocean media, sound speed changes are unavoidable and inevitably reflected in the spatial characteristics of the ocean noise field due to the existence of mesoscale phenomena, such as ocean currents, eddies, tides, and internal waves. In a typical wind-induced noise (an important source of the ocean ambient noise), a surface boundary undergoes fluctuations [19]. Boundary perturbations inevitably affect the spatial characteristics of ocean noise field.

The manner by which the spatial characteristics of the noise field are used in the extraction of water column or sea surface information depends on the influence of the sound speed changes in the water column and sea boundary perturbations.

Using sensitivity kernel in the study of the effects of parameter perturbations on physical quantities is emerging in the field of geophysics [20, 21]. This approach provides a method for analyzing the effects of parameter perturbations on the spatial characteristics of ocean noise fields. In recent years, research on sensitivity kernel has emerged in ocean acoustics. Skarsoulis [22] derived the travel time sensitivity kernel on the basis of Born approximation and analyzed the effects of sound speed changes on travel time. Dzieciuch [23] analyzed the structure and stability of the sensitivity kernel. Notably, the travel time sensitivity kernel has been applied in ocean acoustic tomography.

By using sensitivity kernel to analyze the effects of parameter perturbations on physical quantities, this study derived the surface noise cross-spectral-density sensitivity kernel for sound speed changes and local surface boundary perturbations. Moreover, the effects of parameter perturbations on the physical quantities on surface noise cross-spectral density function and noise intensity were analyzed.

## SURFACE NOISE CROSS-SPECTRAL DENSITY

In the marine medium shown in Fig. 1, ambient noise is generated by wind-induced breaking waves and rainfall. Assuming that the monopole noise sources are uniformly distributed in the infinite horizontal plane with a depth of  $z_s$ , we denote the random surface noise source term as  $S(\mathbf{r}_s)$  [24], where  $\mathbf{r}_s$  denotes the vector from the noise source point to the receiver;  $\rho_1$  and  $c_1$  denote the density and sound speed, respectively, of the water column;  $\rho_2$  and  $c_2$  denote the density and sound speed, respectively, of the semi-infinite seabed. According to Green's function solution of sound fields in horizontally stratified media, the velocity potential function of the surface noise field composed of the monopole noise source can be denoted as follows:

$$\varphi(\mathbf{r}, z) = \int d^2\mathbf{r}_s S(\mathbf{r}_s) G(\mathbf{r}, \mathbf{r}_s; z, z_s), \quad (1)$$

where  $G(\mathbf{r}, \mathbf{r}_s; z, z_s)$  denotes the Green's function between the noise source located at  $(\mathbf{r}_s, z_s)$  and the receiver located at  $(\mathbf{r}, z)$ , thereby satisfying the following Helmholtz equation:

$$\left[ \nabla^2 + \frac{\omega^2}{c^2(\mathbf{r}, z)} \right] G(\mathbf{r}, \mathbf{r}_s; z, z_s) = -\delta(\mathbf{r} - \mathbf{r}_s, z - z_s), \quad (2)$$

and the appropriate boundary conditions. The ambient noise cross-spectral density  $\mathbf{C}(\mathbf{r}_1, z_1; \mathbf{r}_2, z_2)$  is defined as follows:

$$\mathbf{C}(\mathbf{r}_1, z_1; \mathbf{r}_2, z_2) = \langle \varphi(\mathbf{r}_1, z_1) \varphi^*(\mathbf{r}_2, z_2) \rangle, \quad (3)$$

where the braces  $\langle \rangle$  denote the statistical average, and the superscript asterisk is the complex conjugation operation. Substituting the velocity potential function of the ocean ambient noise in Eq. (1) into the cross-spectral density in Eq. (3) yields the following:

$$\begin{aligned} \mathbf{C}(\mathbf{r}_1, z_1; \mathbf{r}_2, z_2) &= \langle \varphi(\mathbf{r}_1, z_1) \varphi^*(\mathbf{r}_2, z_2) \rangle \\ &= \left\langle \int d^2 \mathbf{r}_{s1} S(\mathbf{r}_{s1}) G(\mathbf{r}_1, \mathbf{r}_{s1}; z_1, z_{s1}) \right. \\ &\quad \times \left. \int d^2 \mathbf{r}_{s2} S^*(\mathbf{r}_{s2}) G^*(\mathbf{r}_2, \mathbf{r}_{s2}; z_2, z_{s2}) \right\rangle \\ &= \iint d^2 \mathbf{r}_{s1} d^2 \mathbf{r}_{s2} \langle S(\mathbf{r}_{s1}) S^*(\mathbf{r}_{s2}) \rangle \\ &\quad \times G(\mathbf{r}_1, \mathbf{r}_{s1}; z_1, z_{s1}) G^*(\mathbf{r}_2, \mathbf{r}_{s2}; z_2, z_{s1}). \end{aligned} \quad (4)$$

The cross-spectral density  $\langle S(\mathbf{r}_{s1}) S^*(\mathbf{r}_{s2}) \rangle = q^2 N(\boldsymbol{\rho})$  is assumed to be homogeneous and spatially dependent only on the distance  $\boldsymbol{\rho} = \mathbf{r}_{s1} - \mathbf{r}_{s2}$  between the noise sources  $\mathbf{r}_{s1}$  and  $\mathbf{r}_{s2}$ ;  $q$  is the surface source strength.

The strength between the noise sources  $\mathbf{r}_{s1}$  and  $\mathbf{r}_{s2}$  is assumed to be irrelevant, and the cross-spectral density function is related only to the noise source spacing, stated as follows:

$$N(\boldsymbol{\rho}) = 2\delta(\boldsymbol{\rho})/k^2 \rho. \quad (5)$$

Substituting Eq. (5) into Eq. (4) yields the following:

$$\begin{aligned} \mathbf{C}(\mathbf{r}_1, z_1; \mathbf{r}_2, z_2) &= \frac{4\pi q^2}{k^2} \\ &\quad \times \int d^2 \mathbf{r}_s G(\mathbf{r}_1, \mathbf{r}_s; z_1, z_s) G^*(\mathbf{r}_2, \mathbf{r}_s; z_2, z_s). \end{aligned} \quad (6)$$

### CROSS-SPECTRAL DENSITY SENSITIVITY KERNEL FOR SOUND SPEED PERTURBATION

In a real marine medium, the sound speed of a water column is also affected by various natural factors, such as seasons, sunshine, internal waves, and tides. The sound-field Green's function should be first identified to obtain the cross-spectral density function representation of the surface noise field under the sound speed perturbation. According to the first order Born approximation, a disturbance of the sound speed distribution by  $\Delta c$  causes a perturbation in the Green's function  $\Delta G$ . The perturbed Green's function  $G_0 + \Delta G$  satisfies the following equation:

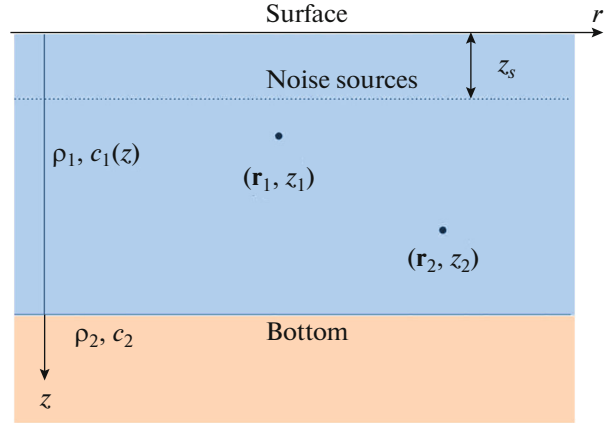


Fig. 1. Surface noise model in horizontally stratified media.

$$\begin{aligned} &\left[ \nabla^2 + \frac{\omega^2}{[c(\mathbf{r}, z) + \Delta c(\mathbf{r}, z)]^2} \right] \\ &\times [G(\mathbf{r}, z | \mathbf{r}_s, z_s) + \Delta G(\mathbf{r}, z | \mathbf{r}_s, z_s)] \\ &= -\delta(\mathbf{r} - \mathbf{r}_s, z - z_s). \end{aligned} \quad (7)$$

By subtracting Eq. (7) from Eq. (2) and adding the term  $\omega^2 \Delta G / c^2$  to both sides, the following equation is obtained:

$$\begin{aligned} &\left[ \nabla^2 + \frac{\omega^2}{c^2(\mathbf{r}, z)} \right] \Delta G(\mathbf{r}, z | \mathbf{r}_s, z_s) \\ &= - \left[ \frac{\omega^2}{[c(\mathbf{r}, z) + \Delta c(\mathbf{r}, z)]^2} - \frac{\omega^2}{c^2(\mathbf{r}, z)} \right] \\ &\times [G(\mathbf{r}, z | \mathbf{r}_s, z_s) + \Delta G(\mathbf{r}, z | \mathbf{r}_s, z_s)]. \end{aligned} \quad (8)$$

The disturbance satisfies the same boundary/interface/radiation conditions according to the unperturbed Green's function. Hence, the integral representation can be used by considering the right-hand side of Eq. (8) as a function of  $\mathbf{r}$  to be the source term.

$$\begin{aligned} \Delta G(\mathbf{r}, z | \mathbf{r}_s, z_s) &= \iiint_V G(\mathbf{r}, z | \mathbf{r}', z') \\ &\times \left[ \frac{\omega^2}{[c(\mathbf{r}', z') + \Delta c(\mathbf{r}', z')]^2} - \frac{\omega^2}{c^2(\mathbf{r}', z')} \right] \\ &\times [G(\mathbf{r}', z' | \mathbf{r}_s, z_s) + \Delta G(\mathbf{r}', z' | \mathbf{r}_s, z_s)] dV(\mathbf{r}', z'). \end{aligned} \quad (9)$$

By retaining the terms of the first order, the following approximation for the perturbation of the Green's function is obtained:

$$\begin{aligned} &\Delta G(\mathbf{r}, z | \mathbf{r}_s, z_s) \\ &= -2\omega^2 \iiint_V G(\mathbf{r}', z' | \mathbf{r}_s, z_s) G(\mathbf{r}, z | \mathbf{r}', z') \\ &\quad \times \frac{\Delta c(\mathbf{r}', z')}{c^3(\mathbf{r}', z')} dV(\mathbf{r}', z'). \end{aligned} \quad (10)$$

The perturbed Green's function  $G$  is as follows:

$$\begin{aligned} G(\mathbf{r}_1, \mathbf{r}_s; z_1, z_s) &= G_0(\mathbf{r}_1, \mathbf{r}_s; z_1, z_s) + \Delta G(\mathbf{r}_1, \mathbf{r}_s; z_1, z_s) \\ &= G_0(\mathbf{r}_1 | \mathbf{r}_s) - 2\omega^2 \iiint_V G(\mathbf{r}', z' | \mathbf{r}_s, z_s) G(\mathbf{r}, z | \mathbf{r}', z') \\ &\quad \times \frac{\Delta c(\mathbf{r}', z')}{c^3(\mathbf{r}', z')} dV(\mathbf{r}', z'). \end{aligned} \quad (11)$$

Substitution of Eq. (11) into the integral term in Eq. (6) yields the following equation:

$$\begin{aligned} &G(\mathbf{r}_1, \mathbf{r}_s; z_1, z_s) G^*(\mathbf{r}_2, \mathbf{r}_s; z_2, z_s) \\ &= (G_0(\mathbf{r}_1, \mathbf{r}_s; z_1, z_s) + \Delta G(\mathbf{r}_1, \mathbf{r}_s; z_1, z_s)) \\ &\quad \times (G_0^*(\mathbf{r}_2, \mathbf{r}_s; z_2, z_s) + \Delta G^*(\mathbf{r}_2, \mathbf{r}_s; z_2, z_s)). \end{aligned} \quad (12)$$

By ignoring the terms of the second-order perturbation  $\Delta G(\mathbf{r}_1, \mathbf{r}_s; z_1, z_s) \Delta G^*(\mathbf{r}_2, \mathbf{r}_s; z_2, z_s)$  and retaining those of the first order of the sound-field Green's function, the following equation is obtained:

$$\begin{aligned} &\Delta(G(\mathbf{r}_1, \mathbf{r}_s; z_1, z_s) G^*(\mathbf{r}_2, \mathbf{r}_s; z_2, z_s)) \\ &= G_0(\mathbf{r}_1, \mathbf{r}_s; z_1, z_s) \Delta G^*(\mathbf{r}_2, \mathbf{r}_s; z_2, z_s) \\ &\quad + G_0^*(\mathbf{r}_2, \mathbf{r}_s; z_2, z_s) \Delta G(\mathbf{r}_1, \mathbf{r}_s; z_1, z_s). \end{aligned} \quad (13)$$

The perturbed cross-spectral density function representation of the surface noise field under the sound speed perturbation can be obtained by combining Eqs. (13) and (6) as follows:

$$\begin{aligned} \Delta \mathbf{C}(\mathbf{r}_1, z_1; \mathbf{r}_2, z_2) &= \frac{4\pi q^2}{k^2} \\ &\quad \times \int (G_0(\mathbf{r}_1, \mathbf{r}_s; z_1, z_s) \Delta G^*(\mathbf{r}_2, \mathbf{r}_s; z_2, z_s) \\ &\quad + G_0^*(\mathbf{r}_2, \mathbf{r}_s; z_2, z_s) \Delta G(\mathbf{r}_1, \mathbf{r}_s; z_1, z_s)) d^2 \mathbf{r}_s. \end{aligned} \quad (14)$$

An integral relation expressing the cross-spectral density perturbation  $\Delta \mathbf{C}(\mathbf{r}_1, z_1; \mathbf{r}_2, z_2)$  in accordance with the underlying sound speed variation  $\Delta c_1(\mathbf{r}')$  is as follows:

$$\begin{aligned} \Delta \mathbf{C}(\mathbf{r}_1, z_1; \mathbf{r}_2, z_2) &= \iiint_V \Delta c_1(\mathbf{r}', z') K_C(\mathbf{r}', z') dV(\mathbf{r}', z'), \end{aligned} \quad (15)$$

where the kernel in the volume integral is the surface noise cross-spectral density sensitivity and is expressed by Eq. (16):

$$\begin{aligned} K_C(\mathbf{r}'; \mathbf{r}_1, z_1; \mathbf{r}_2, z_2) &= \frac{-8\pi q^2 \omega^2}{k^2} \\ &\quad \times \int (G_0(\mathbf{r}_1 | \mathbf{r}') G_0(\mathbf{r}' | \mathbf{r}_s) G_0^*(\mathbf{r}_2, \mathbf{r}_s; z_2, z_s) \\ &\quad + G_0(\mathbf{r}_1, \mathbf{r}_s; z_1, z_s) G_0^*(\mathbf{r}_2 | \mathbf{r}') G_0^*(\mathbf{r}' | \mathbf{r}_s)) \frac{1}{c_1^3(\mathbf{r}')} d^2 \mathbf{r}_s. \end{aligned} \quad (16)$$

The linear operator (Eq. (15)) resulting from the first-order Born approximation is the Fréchet derivative of the cross-spectral density with respect to the

sound speed distribution. Based on Eq. (15), the kernel  $K_C(\mathbf{r}'; \mathbf{r}_1, z_1; \mathbf{r}_2, z_2)$  provides a quantitative description of the cross-spectral density sensitivity  $\mathbf{C}(\mathbf{r}_1, z_1; \mathbf{r}_2, z_2)$  to sound speed changes  $\Delta c_1(\mathbf{r}')$  at any 3D location within the acoustic waveguide.

### CROSS-SPECTRAL DENSITY SENSITIVITY KERNEL FOR SURFACE SCATTERING

Sea surface undulation is inevitable, considering the ambient noise generated by wind-induced breaking waves and rainfall. The propagation from a source at  $\mathbf{r}_s$  to a field point at  $\mathbf{r}$  for the unperturbed waveguide is presented by the Green's function  $G_0$  at the frequency  $\omega$ .

The perturbed Green's function is changed into  $G(\mathbf{r}, \mathbf{r}_s; z, z_s)$  when a local perturbation  $\Delta h$  is generated at the air–water interface. The following equation is obtained for a set of points  $\mathbf{r}'$  located at the air–water interface by applying the Green theorem in the frame of the first-order scattering Born approximation:

$$\begin{aligned} G(\mathbf{r}, \mathbf{r}_s; z, z_s) &= G_0(\mathbf{r}, \mathbf{r}_s; z, z_s) \\ &\quad + \Delta G(\mathbf{r}, \mathbf{r}_s; z, z_s) = G_0(\mathbf{r}, \mathbf{r}_s; z, z_s) \\ &\quad - \oint \nabla_n G_0(\mathbf{r}, \mathbf{r}'; z, 0) \Delta h(\mathbf{r}') \nabla_n G_0(\mathbf{r}', \mathbf{r}_s; 0, z_s) dS. \end{aligned} \quad (17)$$

The following integral relation expressing the cross-spectral density perturbation  $\Delta \mathbf{C}(\mathbf{r}_1, z_1; \mathbf{r}_2, z_2)$  in accordance with the underlying local air–water interface perturbation  $\Delta h(\mathbf{r}')$  is obtained by substituting the perturbation in the Green's function by  $\Delta G$  into Eq. (14):

$$\Delta \mathbf{C}(\mathbf{r}_1, z_1; \mathbf{r}_2, z_2) = \oint \Delta h(\mathbf{r}') K_h(\mathbf{r}') dS, \quad (18)$$

where the kernel in the volume integral is the surface noise cross-spectral density sensitivity for surface scattering and is expressed by Eq. (19):

$$\begin{aligned} K_h(\mathbf{r}'; \mathbf{r}_1, z_1; \mathbf{r}_2, z_2) &= -\frac{4\pi q^2}{k^2} \\ &\quad \times \int (G_0(\mathbf{r}_1, \mathbf{r}_s; z_1, z_s) \nabla_n G_0^*(\mathbf{r}_2, \mathbf{r}'; z, 0) \\ &\quad \times \nabla_n G_0^*(\mathbf{r}', \mathbf{r}_s; 0, z_s) + G_0^*(\mathbf{r}_2, \mathbf{r}_s; z_2, z_s) \\ &\quad \times \nabla_n G_0(\mathbf{r}_1, \mathbf{r}'; z, 0) \nabla_n G_0(\mathbf{r}', \mathbf{r}_s; 0, z_s)) d^2 \mathbf{r}_s. \end{aligned} \quad (19)$$

The linear operator (Eq. (18)) resulting from the first-order Born approximation is the Fréchet derivative of the cross-spectral density with respect to the local air–water interface perturbation distribution. Based on Eq. (18), the kernel  $K_h(\mathbf{r}'; \mathbf{r}_1, z_1; \mathbf{r}_2, z_2)$  provides a quantitative description of the cross-spectral density sensitivity  $\mathbf{C}(\mathbf{r}_1, z_1; \mathbf{r}_2, z_2)$  to the local air–water interface perturbation  $\Delta h(\mathbf{r}')$  at any 3D location within the acoustic waveguide.

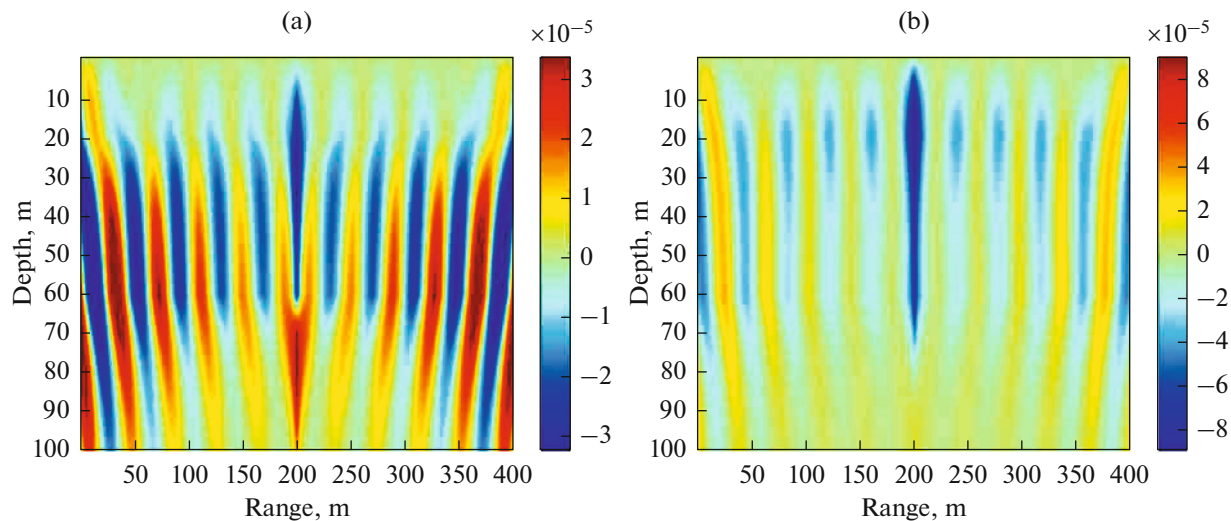


Fig. 2. (a)—Real and (b)—imaginary parts of cross-spectral density sensitivity kernel at frequency of 20 Hz.

Notably, the noise-intensity sensitivity kernel can be obtained by setting  $z = z_1 = z_2$  and  $\mathbf{r} = \mathbf{r}_1 = \mathbf{r}_2$  in the expression of the surface noise cross-spectral density sensitivity kernel. Fundamentally, the cross-spectral density sensitivity kernel is complex, whereas the noise intensity sensitivity kernel is real.

The present derivation for the cross-spectral density sensitivity kernel is based on the first Born (weak scattering) approximation, which comprises reliable cases of small perturbations. It is also called the single- or weak-scattering approximation, or wave-field linearization. Some literatures [25] show that when the sound speed disturbance is less than 2%, the difference of scattering field between based on the second-order Born approximation and based on first-order Born approximation is small so both can be considered identical. When sound speed disturbance is greater than 5%, such difference is relatively large, implying that secondary scattering cannot be ignored. There is another literature [26] that discuss the validity of the linear relation between cross-correlation delay times and velocity model perturbations. Reference [26] shows that the observed cross-correlation delays remain sufficiently linear, depending on frequency, for sharp velocity contrasts of up to 10 per cent in a checkerboard model. Other methods, such as the Rytov approximation, provide a better representation of the transmitted or forward-scattered part of the wave field.

#### NUMERICAL ANALYSIS OF CROSS-SPECTRAL DENSITY SENSITIVITY KERNEL

In this section, we present numerical results for the cross-spectral density sensitivity kernel, assuming the 2D perturbations of a horizontally stratified background medium, as shown in Fig. 1. Hence, wave-number integration techniques (Fast Field Process-

ing) can be applied to provide the unperturbed Green's function. The water depth is 100 m, the water density is  $1000 \text{ kg/m}^3$ , the sound speed of the water column is 1500 m/s, the bottom density is  $1800 \text{ kg/m}^3$ , and the sound speed of an infinite half space is 1600 m/s. Thus, the monopole noise sources are uniformly distributed in an infinite horizontal plane with 1 m depth. The horizontal position of two reference receivers is 200 m, and the depth values of the receivers are 20 and 60 m. And the integration area for sensitivity kernels in numerical simulation is from 0 to 400 m, the step of noise source distribution for integration is 1 m. The numerical results of the cross-spectral density kernel for the sound speed changes and local air-water interface perturbations are shown in sections A and B, respectively.

##### A. Surface Noise Cross-spectral Density Sensitivity Kernel for Sound Speed Changes

Figures 2 to 4 show the distribution of the cross-spectral density sensitivity kernel for sound speed changes ((a) the real and (b) imaginary parts of the sensitivity kernel). As shown in the figures, the perturbations of sound speed in the entire observation plane lead to a change in the surface noise cross-spectral density function because the noise source is distributed in an infinite horizontal plane. The sensitivity kernel at 20 Hz is shown in Fig. 2. The vertical distance between two receivers is less than the wavelength of sound wave. Moreover, as the sound speed of the area between two receivers increases, the real and imaginary parts of the surface noise cross-spectral density function decreases.

The real and imaginary parts of the cross-spectral density sensitivity kernels are symmetric, with alternating negative/positive/zero sensitivity. A positive

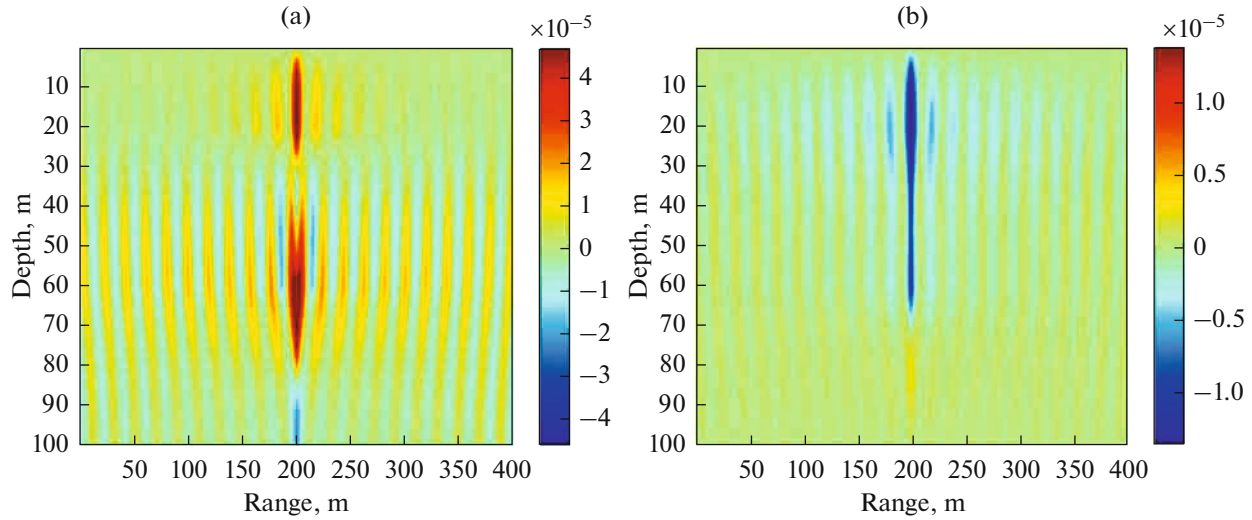


Fig. 3. (a)—Real and (b)—imaginary parts of cross-spectral density sensitivity kernel at frequency of 40 Hz.

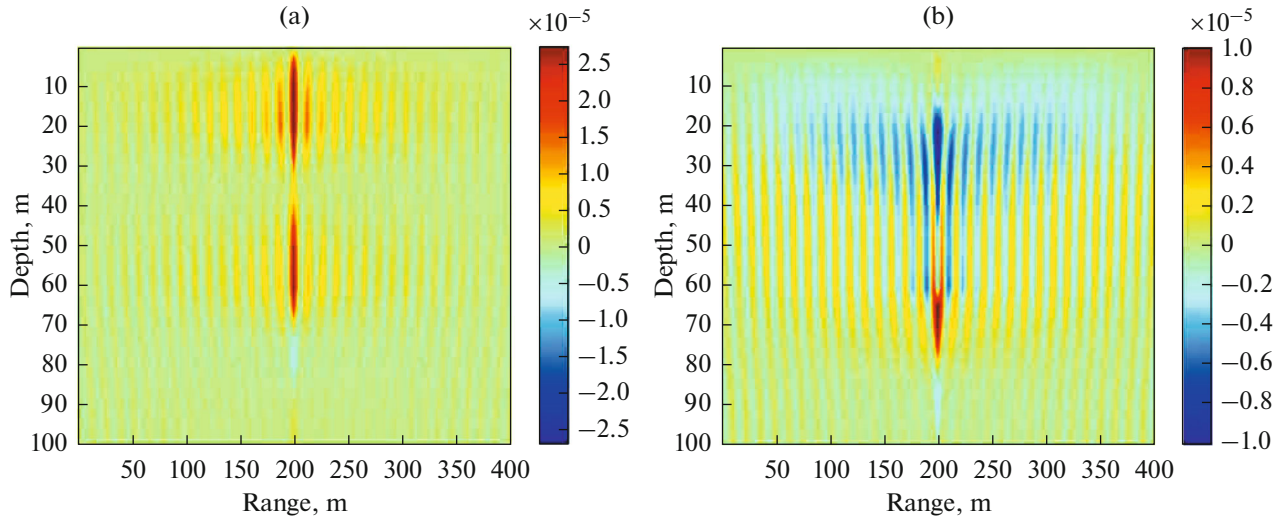


Fig. 4. (a)—Real and (b)—imaginary parts of cross-spectral density sensitivity kernel at frequency of 60 Hz.

value for the real (or imaginary) part of  $K_C(\mathbf{r}')$  at a particular location indicates that as the sound speed increases at that location, the aforementioned section of the cross-spectral density function also increases. Conversely, a negative value for the real (or imaginary) part of  $K_C(\mathbf{r}')$  indicates that as the sound speed decreases, the real (or imaginary) part of the cross-spectral density function also decreases. Finally, a zero indicates that a change in sound speed has no effect on the cross-spectral density function.

Sensitivity kernels at 40 and 60 Hz are shown in Figs. 3 and 4, respectively. The effects of sound speed perturbations on the cross-spectral density function weakens as the distance between two receivers increases.

In the imaginary part of the cross-spectral density function, the influential area of the effective sound speed perturbations near the sea surface (i.e., noise source) is larger than that close to the sea bottom. The higher the surface noise frequency, the weaker the effect of an area far from two receivers. The variation region of the cross-spectral density sensitivity kernel converges to the connection between two receivers, while the frequency is absolutely high.

Figure 5 shows the variation in the cross-spectral density sensitivity kernel along the vertical direction connecting two receivers. Subpanels (a) to (c) of Fig. 5 show the sensitivity kernel with frequencies of 20, 40, and 60 Hz (solid, dashed, and dotted lines, respectively). The blue and red lines denote the real and imaginary parts of the sensitivity kernels, respectively.

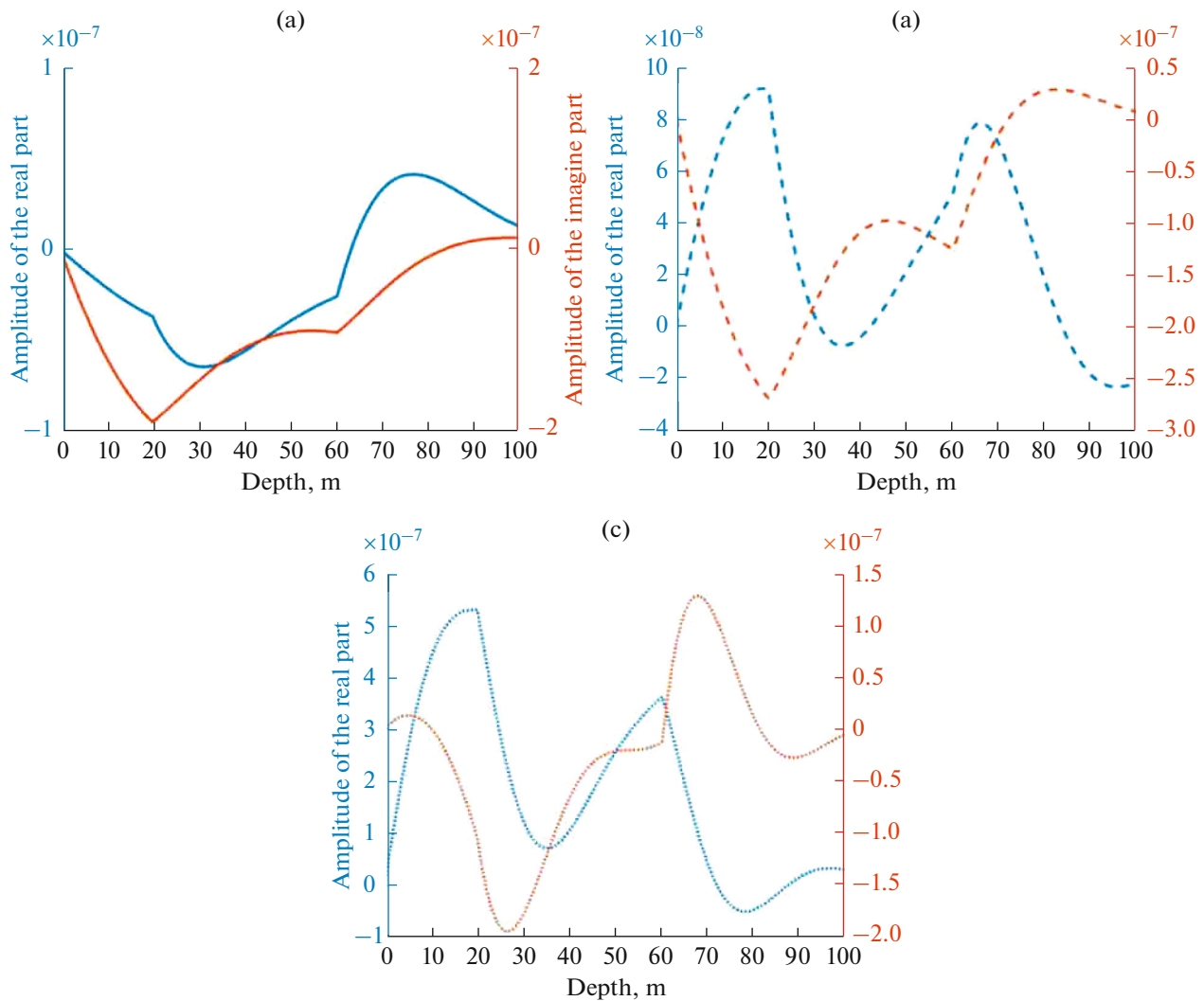


Fig. 5. Variation in cross-spectral density sensitivity kernel with depth at horizontal position of 200 m for different frequencies.

The real part of cross-spectral density sensitivity kernel at 20 Hz is negative among the path connecting two receivers, and the vertical distance between two receivers is less than the wavelength of sound wave. The vertical distance between two receivers is longer than the wavelength of sound wave for 40 and 60 Hz. The real part of the cross-spectral density sensitivity kernel has a minimum point among the paths connecting two receivers, indicating a significant difference from the sensitivity kernel with 20 Hz frequency. The location of the maxima is the position of two receivers.

Figure 6 shows the sensitivity kernels of the horizontal cross-spectral density function for two receivers placed at 30, 50 and 70 m depth with 40 m horizontal distance. It can be found that for two receivers placed with horizontal distance, the peak values of cross-spectral density sensitivity kernels are at the horizontal positions of two receivers. The area in which the sound

speed variations lead significant variations in cross-spectral density function is associated with the depth of two receivers. In addition, the effects of sound speed perturbations on the cross-spectral density function weakens as the distance between two receivers increases.

Figures 7 and 8 show the noise-intensity sensitivity kernel at 20 and 50 m depths, respectively. The noise intensity is influenced by the sound speed changes near the receiver. The sensitivity kernels near the observation point are negative (the blue strip surrounding the observation point) (i.e., as the sound speed increases, the noise intensity decreases). In ray theory, the ray is always bent in a lower sound speed. Thus, when an increase in sound speed is detected near the observation point, the acoustic energy difficultly reaches the observation point, thereby resulting in a decrease in noise intensity.

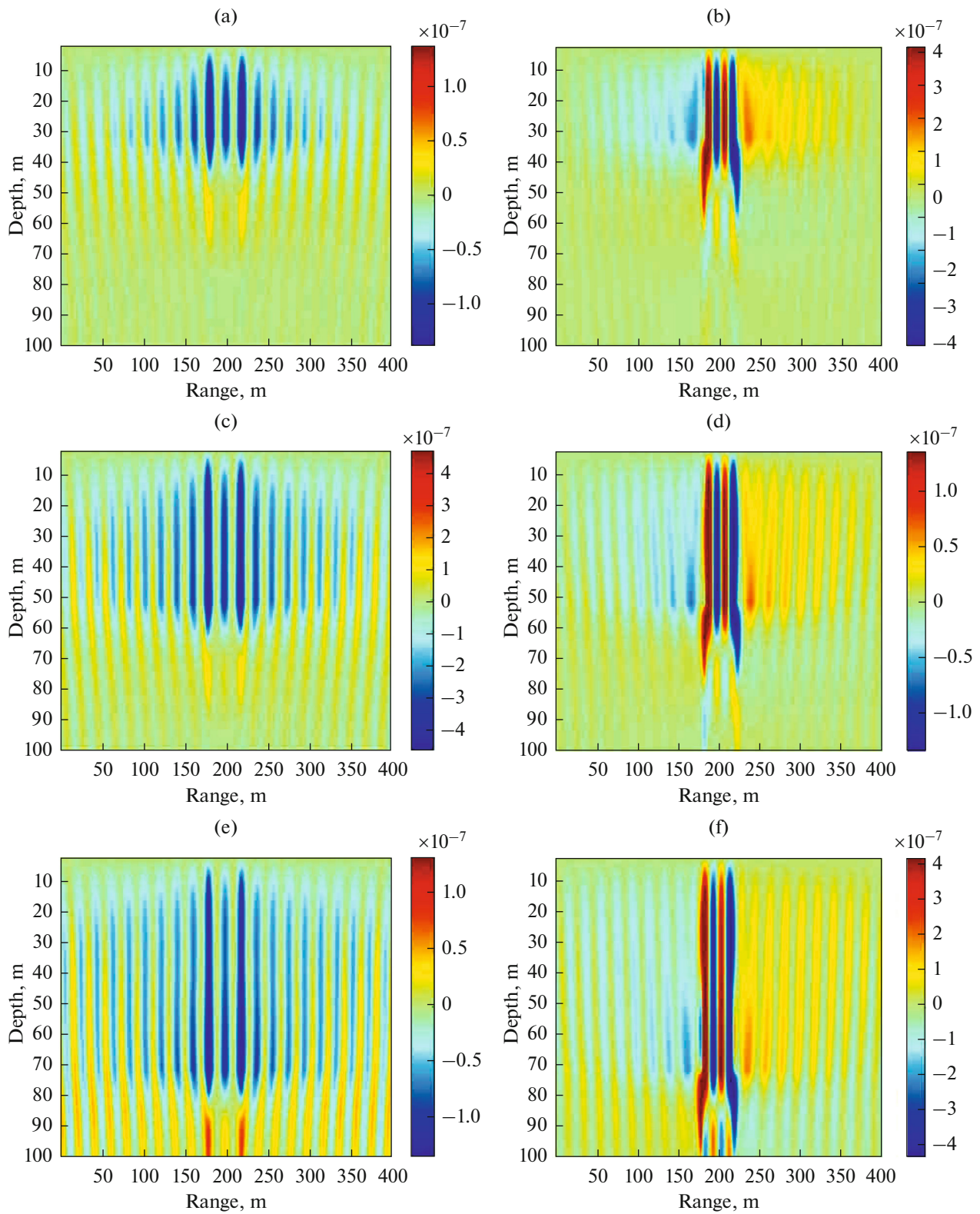


**Fig. 6.** (a, c, e)—Real and (b, d, f)—imaginary parts of horizontal cross-spectral density sensitivity kernel at 40 Hz. Two receivers placed at (a, b)—30 m, (c, d)—50 m, and (e, f)—70 m depth with 40 m horizontal distance.

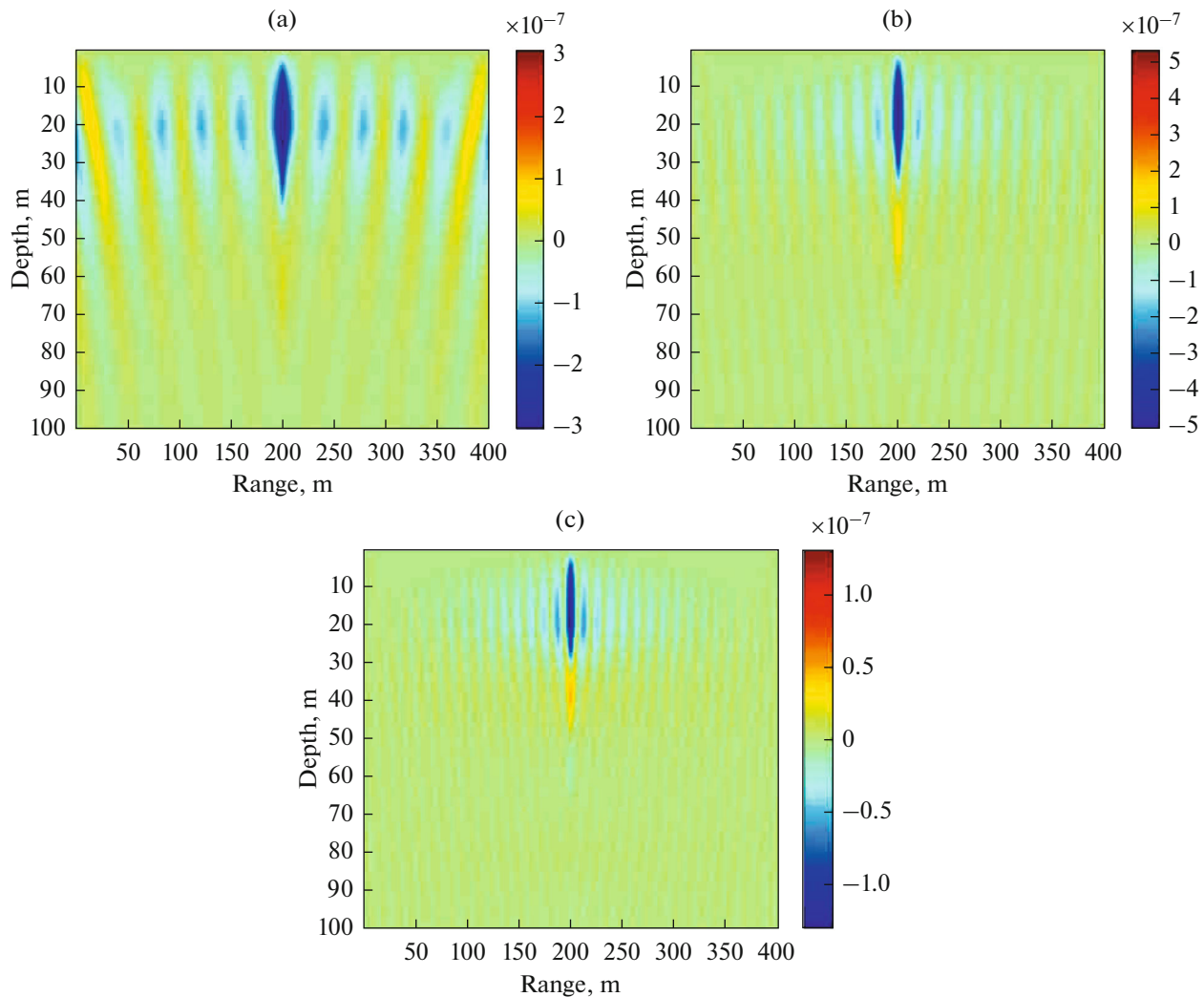


Fig. 7. Noise strength kernel with (a)—20, (b)—40, and (c)—60 Hz frequencies at (200, 20) location.

The blue strip surrounding the observation point is followed by a brightly colored one directly below it. The sound speed increase in this area leads to an enhancement of backscattering at this position, making the noise propagating from the top to the bottom spread to backscatter to the observation point; consequently, the noise intensity increases at this point.

The noise-intensity sensitivity kernels show alternations of negative/positive/zero sensitivity far from the receiver in the horizontal direction. Moreover, the farther the receiver, the weaker the effects of the sound speed perturbations on the noise intensity. A positive value for the noise intensity sensitivity kernel at a particular location indicates that as the sound speed at that location increases, the noise intensity also increases. Meanwhile, a negative value for the noise intensity sensitivity kernel indicates that as the sound speed decreases, the noise intensity also decreases. Finally, a zero indicates that a change in sound speed has no effect on noise intensity. As shown in Fig. 8, the

region affecting the noise intensity at 50 m depth is mainly between the depths of the observation point and the noise source. The lower the frequency and the longer the wavelength of the sound wave, the wider the region.

#### B. Surface Noise Cross-spectral Density Sensitivity Kernel for Surface Scattering

Figure 9 shows the surface noise cross-spectral density sensitivity kernel for surface scattering, where the lateral and vertical axes represent the horizontal position of the boundary perturbation on the sea surface and (a) the real and (b) imaginary parts of the cross-spectral density sensitivity kernel, respectively.

For the noise cross-spectral density of two receivers in the vertical direction, the boundary perturbation directly above two receivers has the greatest influence on the cross-spectral density function. The cross-spectral density sensitivity kernel for surface scattering

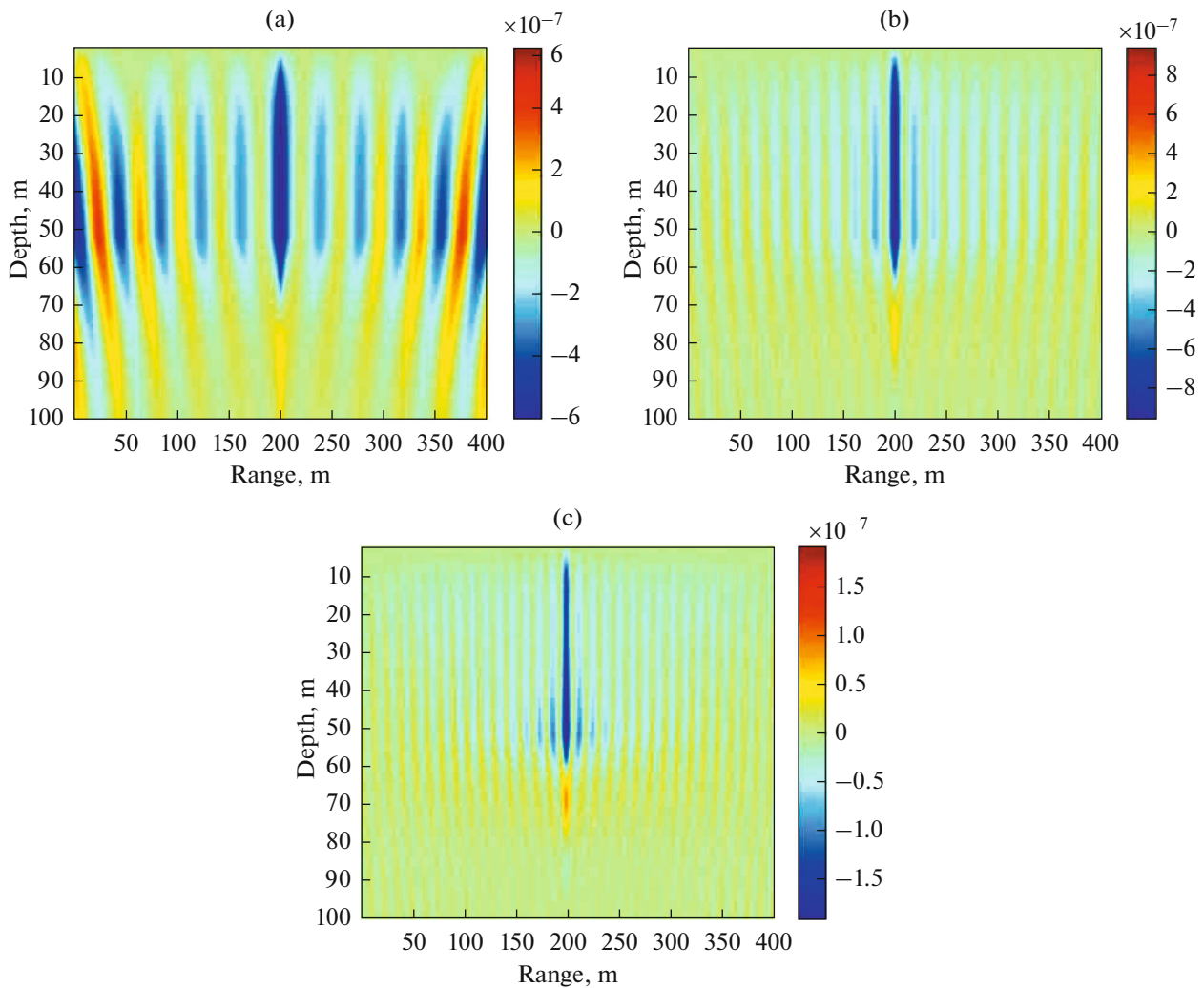


**Fig. 8.** Noise strength sensitivity kernel with (a)—20, (b)—40, and (c)—60 Hz frequencies at (200, 50) location.

oscillates, and the influence of boundary perturbation on the cross-spectral density function gradually weakens when the boundary of the horizontal-direction perturbation is far from two receivers. Moreover, the period of oscillations of the cross-spectral density sensitivity kernel is half the wavelength of the sound wave.

Figure 10 shows the noise-intensity sensitivity kernels for surface scattering with (a) 20, (b) 50, and (c) 80 m depths. The values of the sensitivity kernels in the area directly above the receiver are negative, indicating that the positive perturbation of the upper boundary of the receiver eventually results in a decline in noise intensity. The reason is that the positive perturbation indicates that the surface boundary is far from the receiver, and the noise energy from the noise source to the receiving point is weakened, thereby deteriorating the total noise energy.

In Fig. 10a the receiver depth is 20 m. The oscillating amplitude of the noise intensity sensitivity kernel increases with frequency. Specifically, the influence of

the sea surface disturbance on the noise intensity increases with frequency, and the acoustic wavelength of this frequency is longer than the distance from the receiver to the sea surface. In Fig. 10b the receiver depth is 50 m, and the oscillating amplitude values of the kernels with 30, 40, and 60 Hz frequencies are nearly equal. In Fig. 10c the receiver depth is 80 m. In this case, the oscillating amplitude of the noise-intensity sensitivity kernel decreases at increasing frequency. Specifically, the influence of the sea surface disturbance on the noise intensity weakens when frequency increases, and the acoustic wavelengths of these frequencies are shorter than the distance from the receiver to the sea surface. Therefore, when the acoustic wavelength is longer than the receiver depth, frequency increases and the influence of the sea surface disturbance on the noise intensity increases. When the acoustic wavelength is shorter than the receiver depth, frequency decreases and the influence

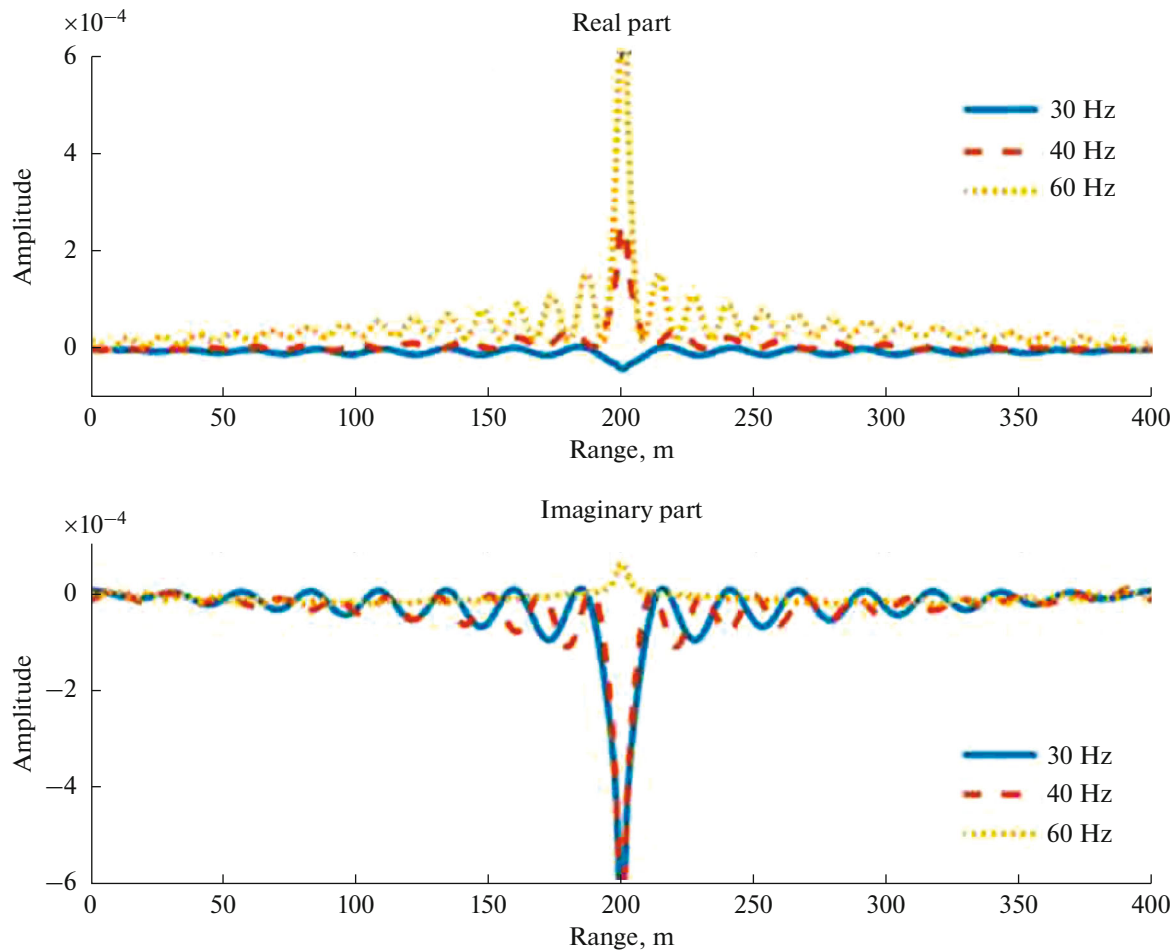


Fig. 9. Surface noise cross-spectral density sensitivity kernel for surface scattering.

of the sea surface disturbance on noise intensity increases.

Figure 11 shows the sensitivity kernels of the horizontal cross-spectral density function. The real parts of the kernels are symmetric with the center position of the path connecting two receivers. The perturbation of the upper surface boundary between two receivers has the greatest influence on the real parts of the cross-spectral density function.

When the boundary perturbation is far from two receivers along the horizontal direction, the cross-spectral density sensitivity kernel for surface scattering oscillates, and the influence of boundary perturbation on the cross-spectral density function gradually weakens. Moreover, the period of the cross-spectral density sensitivity kernel oscillations is half the wavelength of the sound wave. However, the mark for the left/right side of the imaginary part is the opposite.

## CONCLUSIONS

An expression that linearly relates sound speed and surface boundary perturbations at the air–water inter-

face to changes in the surface noise cross-spectral density function is derived in a waveguide. Numerical results show some interesting phenomena stated as follows:

(1) The sound speed perturbations of any position in the entire observation plane can change the surface noise cross-spectral density function because the noise source is distributed in an infinite horizontal plane. The sound speed perturbations along the path connecting two receivers have the greatest influence on the cross-spectral density function of the vertical noise field. The influence of the sound speed perturbations on the cross-spectral density function is weakened as two receivers move far from it.

(2) Noise intensity sensitivity kernel decreases at increased sound speed. This increase hinders the entry of sound energy because the ray is always bent in a lower sound speed.

(3) In the noise cross-spectral density of two receivers in the vertical direction, the boundary perturbation directly above two receivers has the greatest influence on cross-spectral density function. The

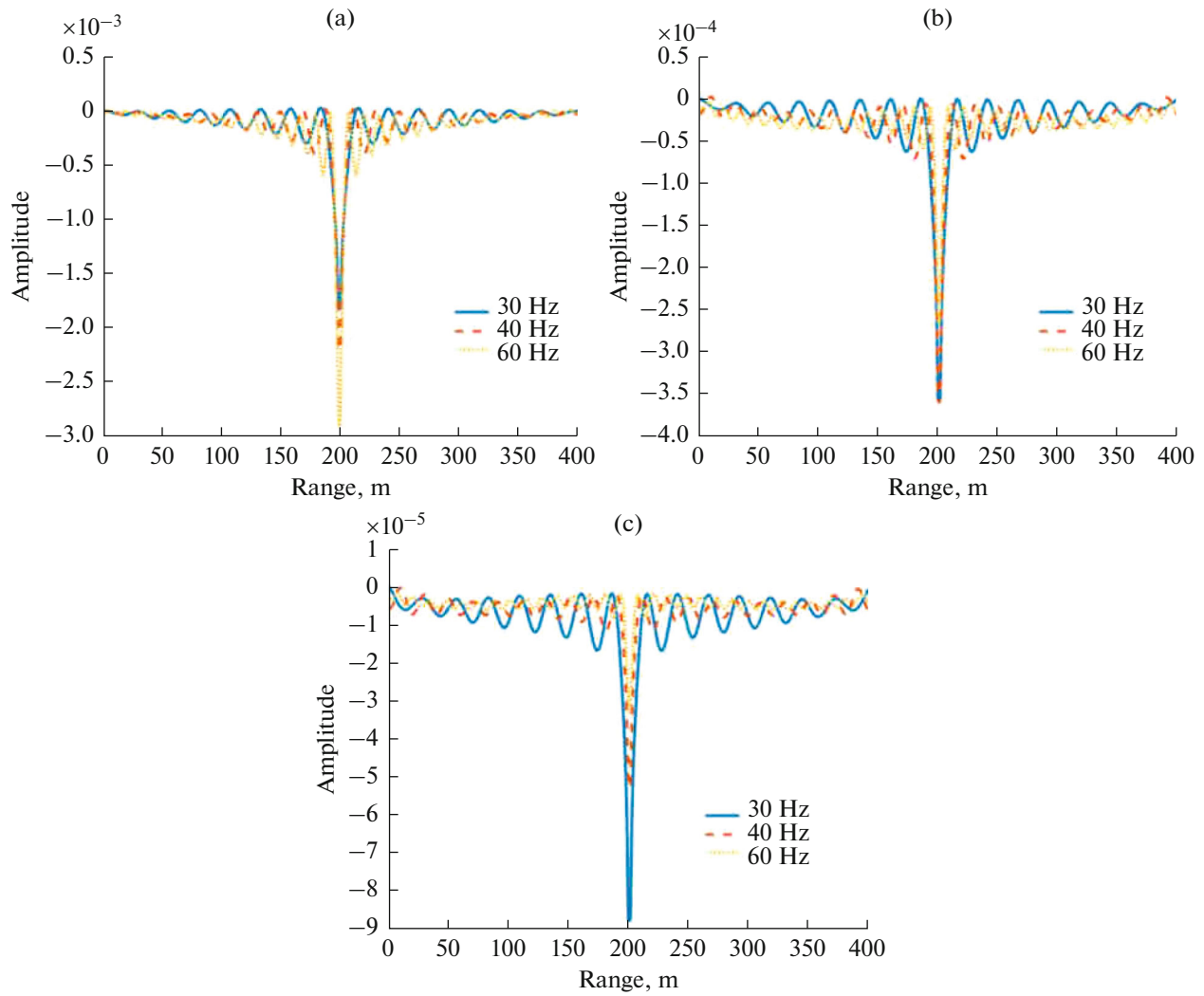


**Fig. 10.** Noise intensity sensitivity kernels for surface scattering with (a)—20, (b)—50, and (c)—80 m depths.

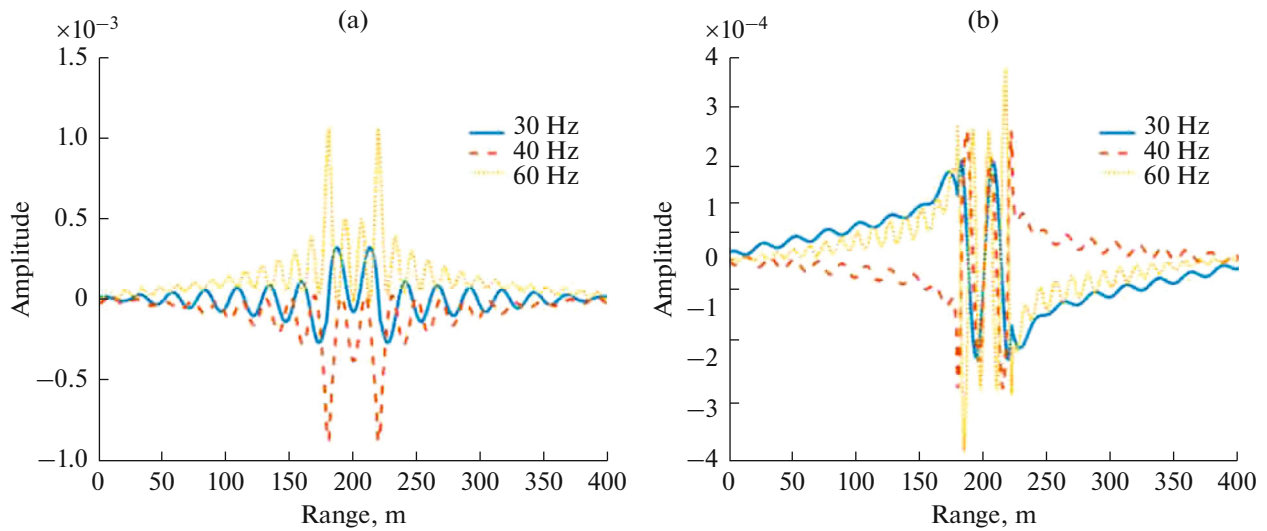


**Fig. 11.** (a)—Real and (b)—imaginary parts of cross-spectral density kernel for two receivers placed at 20 m depth with 40 m horizontal distance.

cross-spectral density sensitivity kernel for surface scattering oscillates, and the influence of boundary perturbation on the cross-spectral density function gradually weakens as the boundary of the horizontal direction perturbation is far from two receivers. Moreover, the period of oscillations on the cross-spectral density sensitivity kernel is half the wavelength of the sound wave, and the positive perturbation of the surface boundary causes the receiver to be far from the surface, thereby resulting in a decrease in the noise intensity.

Although the numerical analysis in this study is limited to a 2D horizontally stratified homogeneous range-independent waveguide, the sensitivity kernels can be extended to arbitrary 3D ocean media, given that the Green's function of sound field in the corresponding medium can be calculated. The cross-spectral density sensitivity kernel presented in this study provides a method for studying the influence of sound speed and local surface boundary perturbations on the cross-spectral density functions of surface noise fields. Finally, the cross-spectral density sensitivity kernel can be used for the inversion of sound speed profiles and boundary perturbations when the cross-spectral density function of ocean ambient noise can be obtained accurately.

#### FUNDING

This work was funded by the National Natural Science Foundation of China (Grant no. 61471327). This work was funded by the National Defense Science and Technology Innovation Zone.

#### REFERENCES

1. X. Y. Guo, F. Li, and P. G. Tie, *Physics* **43**, 723 (2014).
2. V. V. Goncharov, A. S. Shurup, O. A. Godin, N. A. Zabolotin, A. I. Vedenov, S. N. Sergeev, M. G. Brown, and A. V. Shatrin, *Acoust. Phys.* **62**, 436 (2016).
3. B. Y. Yin, E. C. Shang, L. Ma, and J. H. Lin, *Sci. Sin. Phys., Mech. Astron.* **41**, 741 (2011).
4. S. Q. Yu, Y. W. Huang, and Y. Song, *J. Harbin Eng. Univ.* **33**, 828 (2012).
5. C. H. Harrison and D. G. Simons, *J. Acoust. Soc. Am.* **112**, 1377 (2002).
6. D. Arnaud, L. Eric, and T. Mickael, *J. Acoust. Soc. Am.* **113**, 2973 (2003).
7. J. Zhou, S. Qu, K. Piao, K. Iqbal, Y. Dong, S. Zhang, H. Zhang, X. Wang, and Y. Liu, *J. Acoust. Soc. Am.* **142**, EL507 (2017).
8. O. A. Godin, B. G. Katsnelson, J. X. Qin, M. G. Brown, N. A. Zabolotin, and X. Q. Zang, *Acoust. Phys.* **63**, 309 (2017).
9. M. Siderius, C. H. Harrison, and M. B. Porter, *J. Acoust. Soc. Am.* **120**, 1315 (2006).
10. A. I. Khilko, I. P. Smirnov, A. I. Mashonin, and A. V. Shafranyuk, *Acoust. Phys.* **64**, 215 (2018).
11. B. F. Cron and C. H. Sherman, *J. Acoust. Soc. Am.* **34**, 1732 (1962).
12. D. M. Chapman, *J. Acoust. Soc. Am.* **85**, 648 (1989).
13. W. A. Kuperman and F. J. Ingenito, *J. Acoust. Soc. Am.* **67**, 1988 (1980).
14. W. M. Carey, *J. Acoust. Soc. Am.* **80**, 1523 (1986).
15. C. H. Harrison, *J. Acoust. Soc. Am.* **102**, 2655 (1997).
16. M. Siderius, L. Muzi, C. H. Harrison, and P. L. Nielsen, *J. Acoust. Soc. Am.* **133**, EL149 (2013).
17. L. Muzi, M. Siderius, and P. L. Nielsen, *J. Acoust. Soc. Am.* **140**, 1513 (2016).
18. J. E. Quijano, S. E. Dosso, M. Siderius, and L. Muzi, *J. Acoust. Soc. Am.* **135**, EL318 (2014).
19. N. A. Zavolskii, A. I. Malekhanov, M. A. Raevskii, and A. V. Smirnov, *Acoust. Phys.* **63**, 542 (2017).
20. M. Henk, N. Guust, and F. A. Dahlen, *Geophys. J. Int.* **132**, 521 (1998).
21. H. Marquering, F. A. Dahlen, and G. Nolet, *Geophys. J. Int.* **137**, 805 (2002).
22. E. K. Skarsoulis and B. D. Cornuelle, *J. Acoust. Soc. Am.* **116**, 227 (2004).
23. M. A. Dzieciuch, B. D. Cornuelle, and E. K. Skarsoulis, *J. Acoust. Soc. Am.* **134**, 3318 (2013).
24. F. B. Jensen, W. A. Kuperman, M. B. Porter, and H. Schmidt, *Computational Ocean Acoustics*, 2nd ed. (Springer, New York, 2012).
25. X. P. Dong, J. W. Teng, X. Y. Ma, and P. H. Song, *J. Geophysics* **59**, 1070 (2016).
26. G. Mercierat and G. Nolet, *Geophys. J. Int.* **192**, 681 (2013).